

**Plasmonic enhanced furfural hydrogenation catalyzed by stable
carbon coated copper nanoparticles driven from metal-organic
frameworks**

Ruiyi Wang^{a1}, Huan Liu^{a,b1}, Xiaoyu Wang^{a,b}, Xincheng Li^{a,b}, Xianmo Gu^{a*}, Zhanfeng Zheng^{a,b*}

^aState Key Laboratory of Coal Conversion, Institute of Coal Chemistry, Chinese Academy of Sciences, Taiyuan, Shanxi 030001, PR China. Email: zfzheng@sxicc.ac.cn

^bCenter of Materials Science and Optoelectronics Engineering, University of Chinese Academy of Sciences, Beijing 100049, PR China

* Corresponding authors.

E-mail address: zfzheng@sxicc.ac.cn (Z. Zheng); guxm@sxicc.ac.cn (X. Gu).

1 These authors contributed equally to this work.

Table of Contents

Fig. S1 TGA-DTA curves of HKUST-1.....	3
Fig. S2 N ₂ adsorption–desorption isotherms of (a) HKUST-1, (b) Cu/AC (c) Cu ₂ O-Cu@C.	4
Fig. S3 N ₂ adsorption/desorption isotherms and the corresponding BJH pore-size distribution curves of various Cu@C-T samples	5
Fig. S4 Gas chromatographic analysis of gaseous products during pyrolysis of HKUST-1	6
Table S1 Textural properties and compositions of various samples.....	7
Fig. S5 Raman spectrum of various Cu@C-T samples	8
Fig. S6 FT-IR spectrum of various Cu@C-T samples	9
Fig. S7 The DRIFT spectra of FAL absorbed on Cu@C-T catalysts.	10
Fig. S8 Recyclability and stability of Cu@C-600 photocatalyst.....	11
Fig. S9 The output spectra of LED light sources.	12
Fig. S10 UV-vis-DR spectra of various samples.	13
Fig. S11 XRD pattern of Cu/AC.	14

Fig. S1 TGA-DTA curves of HKUST-1

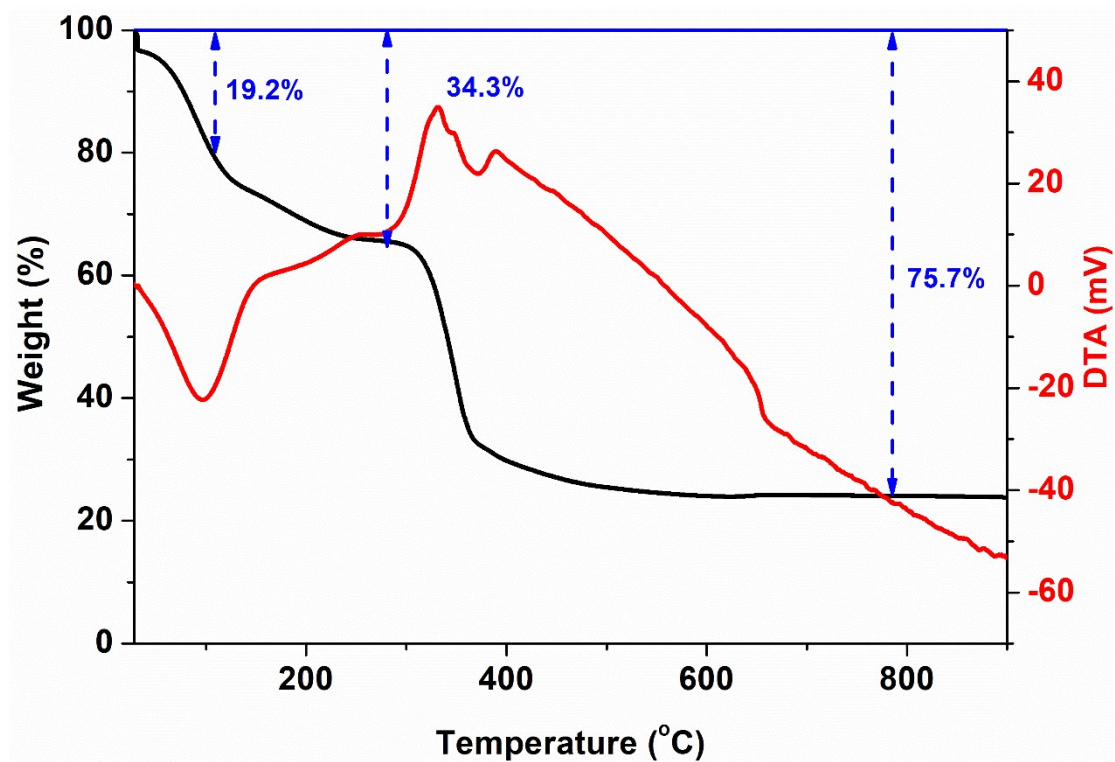


Fig. S1 TGA-DTA curves of HKUST-1

Fig. S2 N₂ adsorption–desorption isotherms of (a) HKUST-1, (b) Cu/AC (c) Cu₂O-Cu@C.

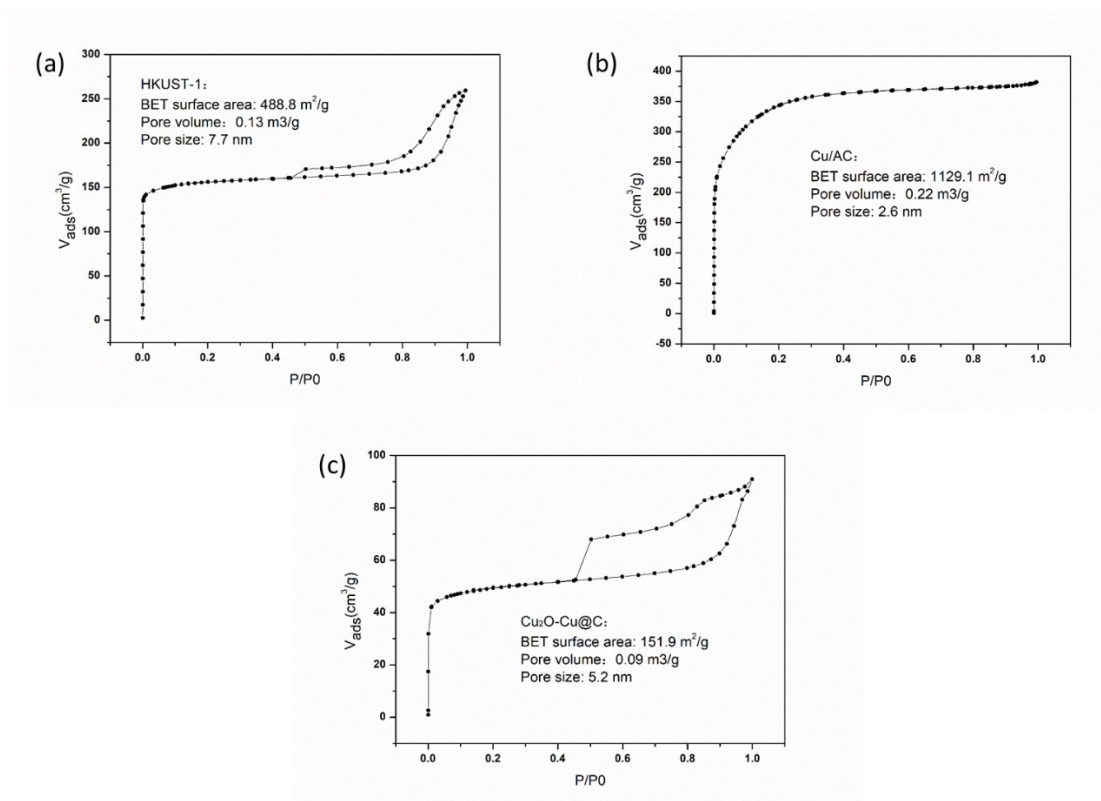


Fig. S2 N₂ adsorption–desorption isotherms of (a) HKUST-1, (b) Cu/AC (c) Cu₂O-Cu@C.

Fig. S3 N₂ adsorption/desorption isotherms and the corresponding BJH pore-size distribution curves of various Cu@C-T samples

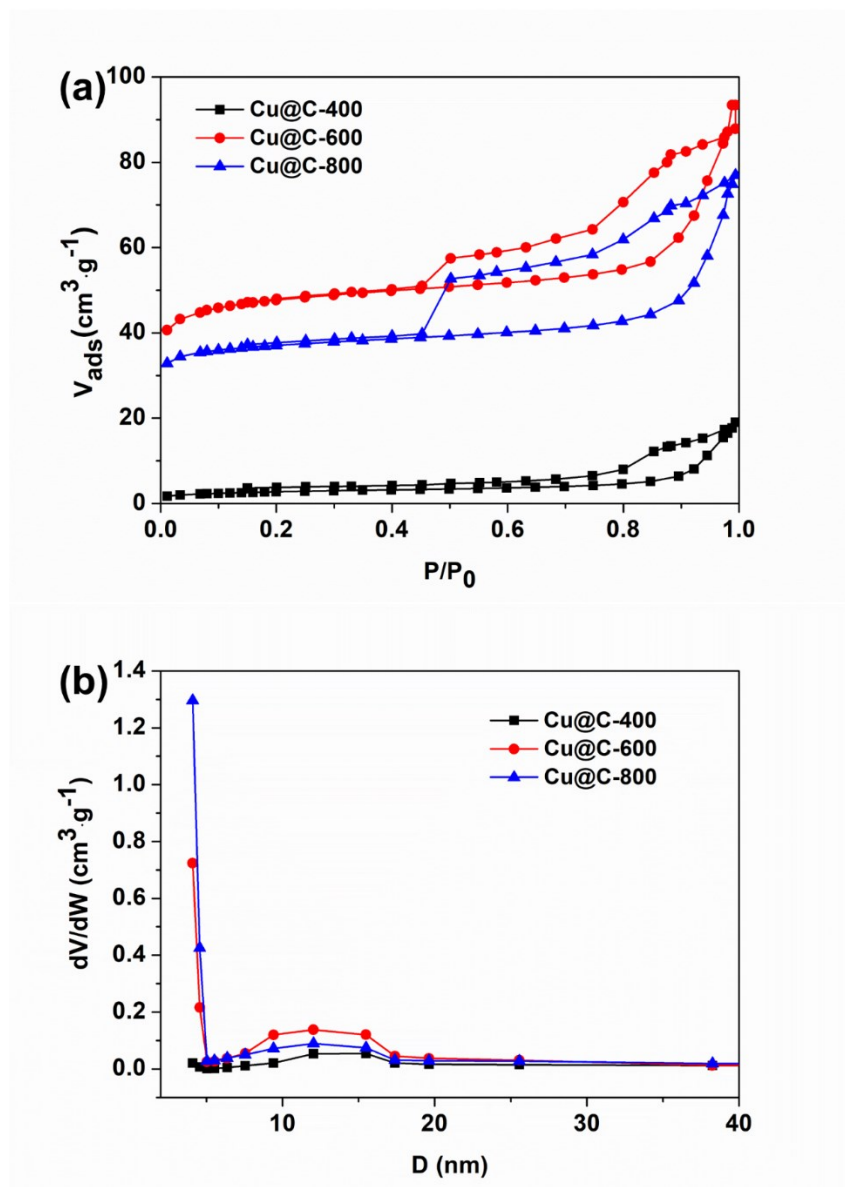


Fig. S3 (a) N₂ adsorption/desorption isotherms and (b) the corresponding BJH pore-size distribution curves of various Cu@C-T samples.

Fig. S4 Gas chromatographic analysis of gaseous products during pyrolysis of HKUST-1

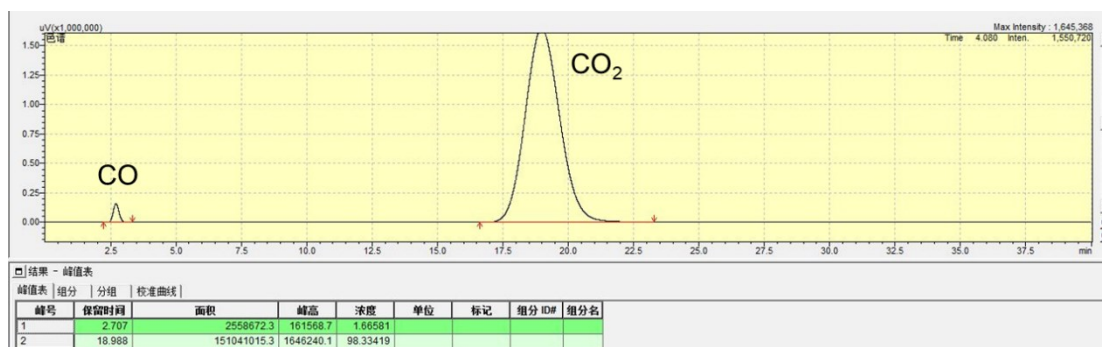


Fig. S4 Gas chromatographic analysis of gaseous products during pyrolysis of HKUST-1.

Table S1 Textural properties and compositions of various samples**Table S1** Textural properties and compositions of various samples

Samples	S_{BET} ($\text{m}^2 \text{g}^{-1}$)	V_{pore} ($\text{cm}^3 \text{g}^{-1}$)	D_{pore} (nm)	Content of elements			
				Cu	C	O	H
Cu@C-400	9.6	0.029	17.4	52.2	31.9	14.3	1.6
Cu@C-600	154.7	0.079	9.0	53.4	32.4	13.0	1.3
Cu@C-800	119.4	0.069	13.1	54.6	33.6	11.0	0.7

Fig. S5 Raman spectrum of various Cu@C-T samples

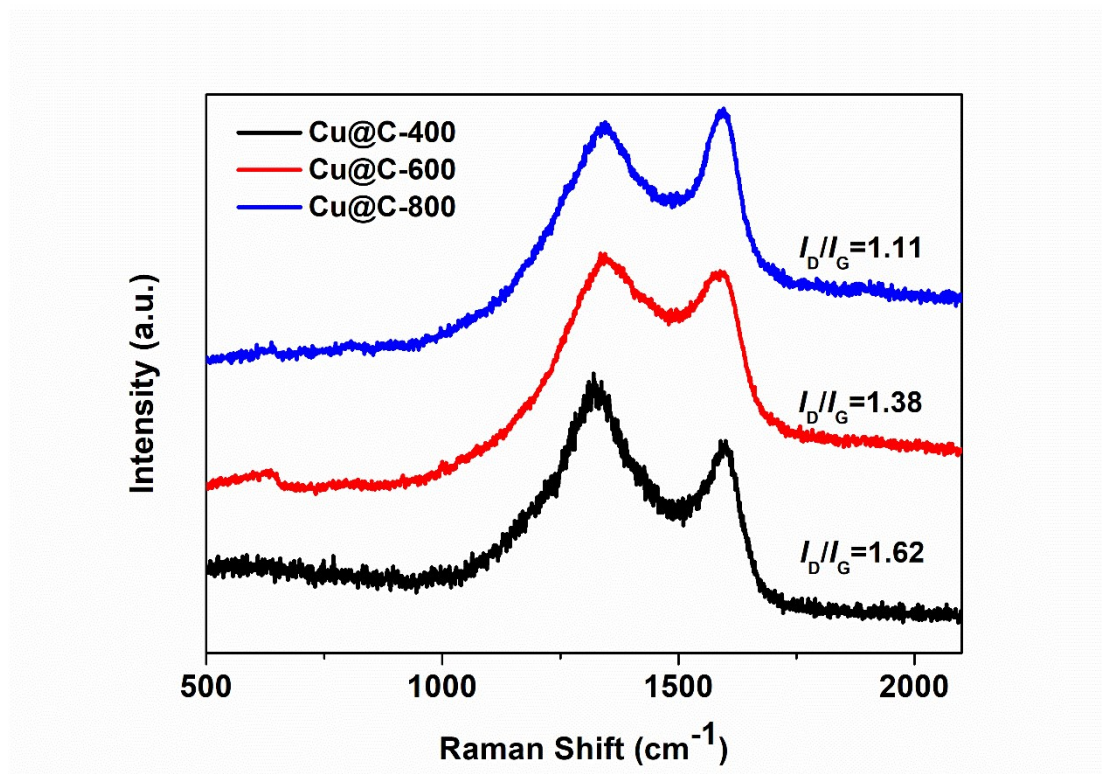


Fig. S5 Raman spectrum of various Cu@C-T samples.

Fig. S6 FT-IR spectrum of various Cu@C-T samples

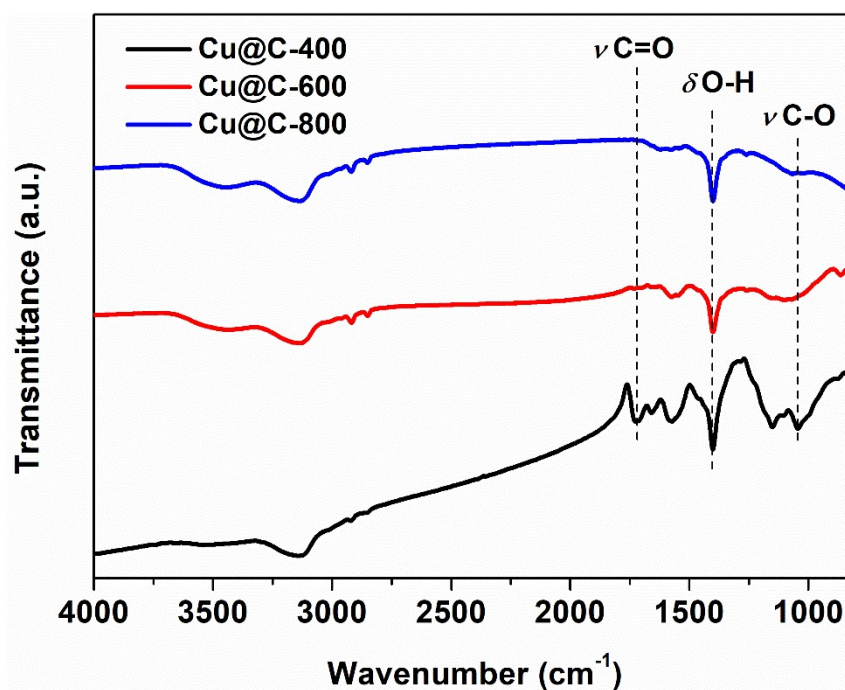


Fig. S6 FT-IR spectrum of various Cu@C-T samples.

Fig. S7 The DRIFT spectra of FAL absorbed on Cu@C-T catalysts.

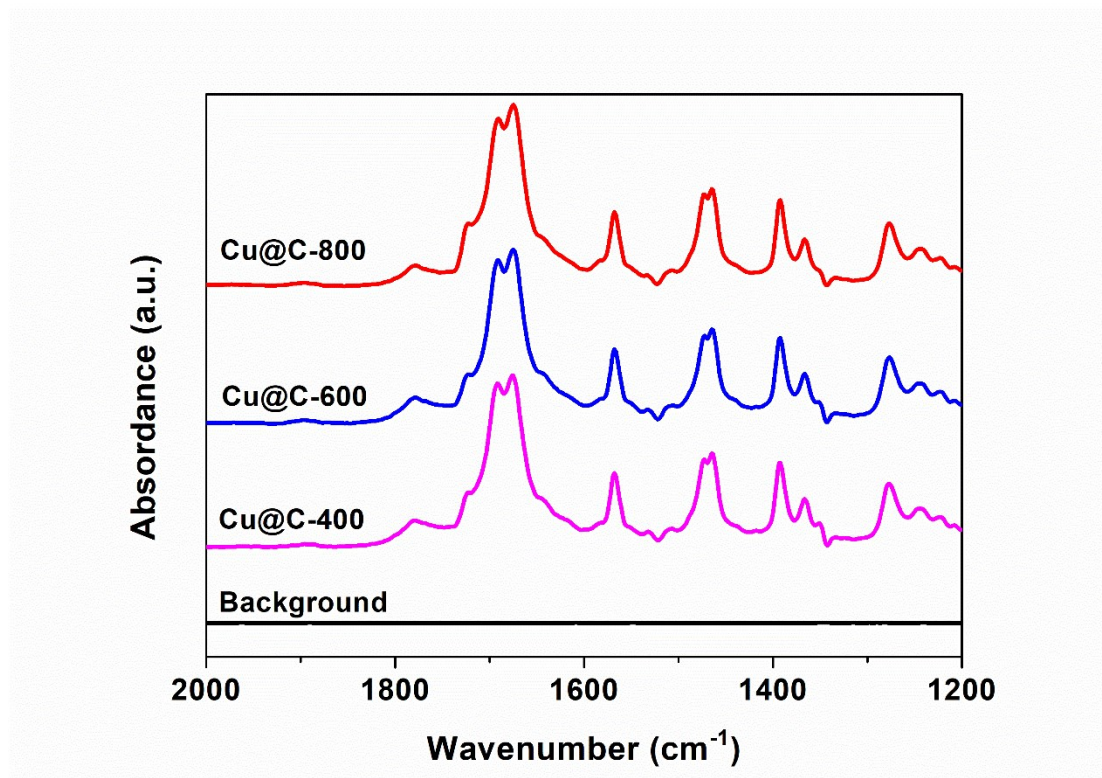


Fig. S7 The DRIFT spectra of FAL absorbed on Cu@C-T catalysts.

Fig. S8 Recyclability and stability of Cu@C-600 photocatalyst.

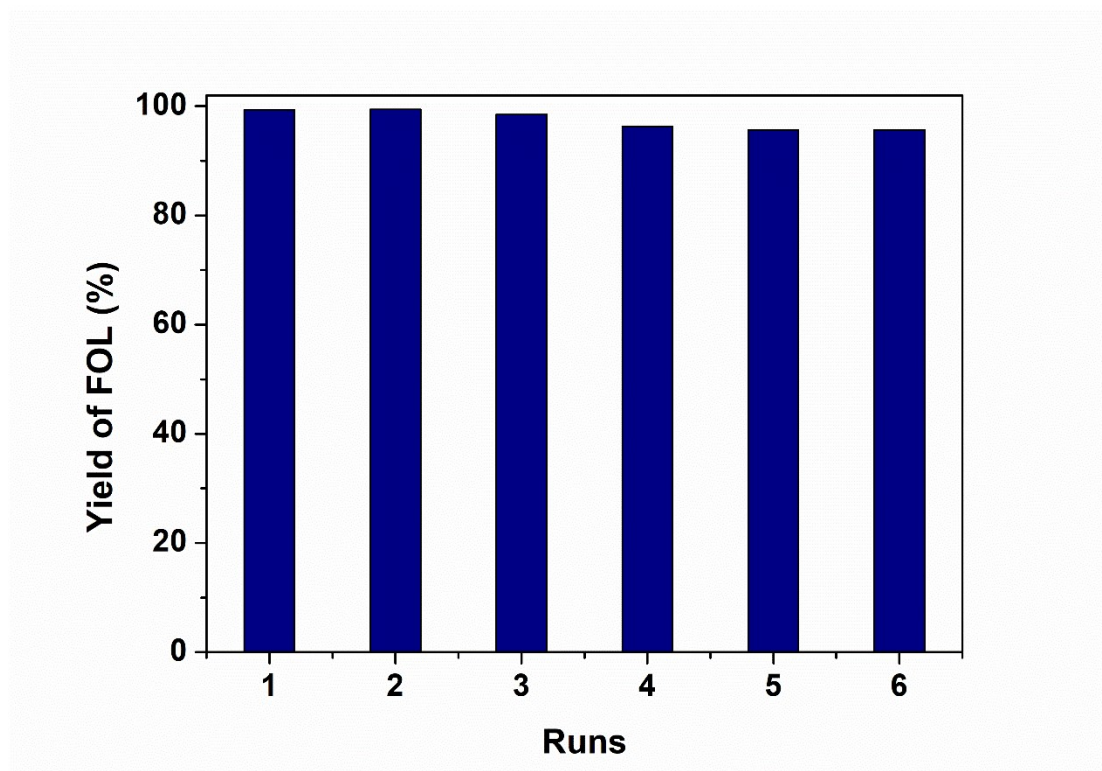


Fig. S8 Recyclability and stability of Cu@C-600 photocatalyst. Reaction conditions: 30 mg of catalyst, 0.2 mmol of substrate, and 5 mL of isopropanol as solvent, 1 atm H₂. The reaction mixture was stirred under visible light irradiation (0.5 W/cm²) at 100 °C for 24 h.

Fig. S9 The output spectra of LED light sources.

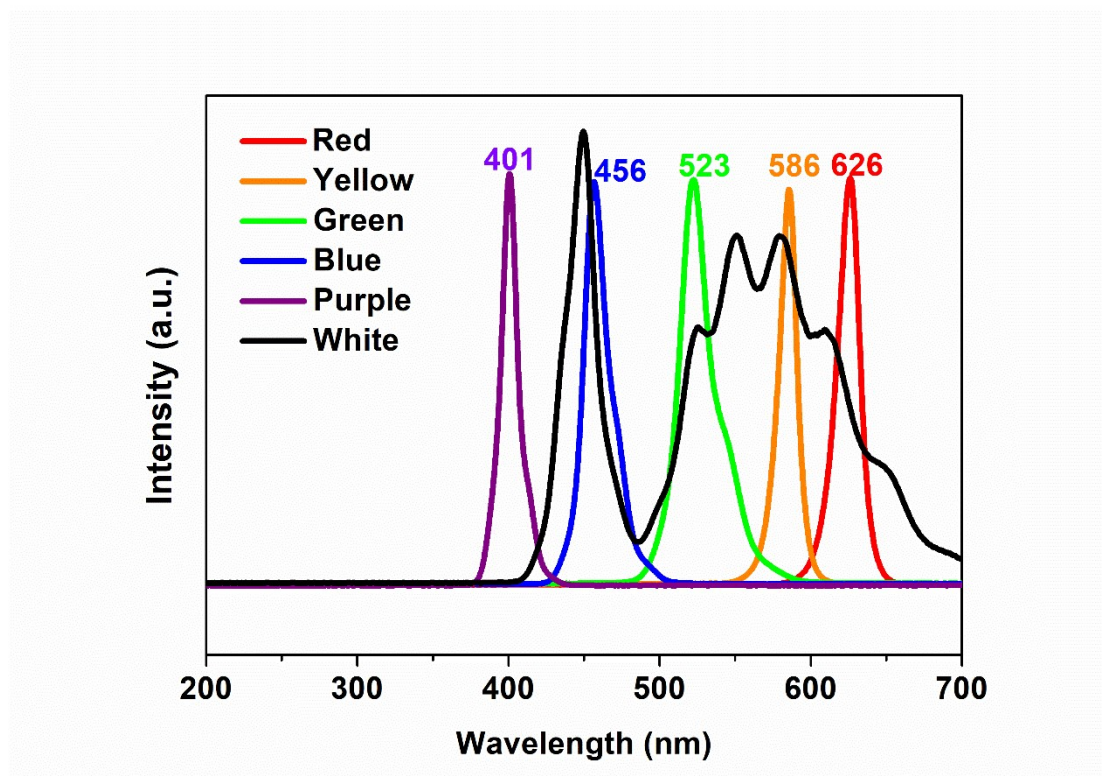


Fig. S9 The output spectra of LED light sources.

Fig. S10 UV-vis-DR spectra of various samples.

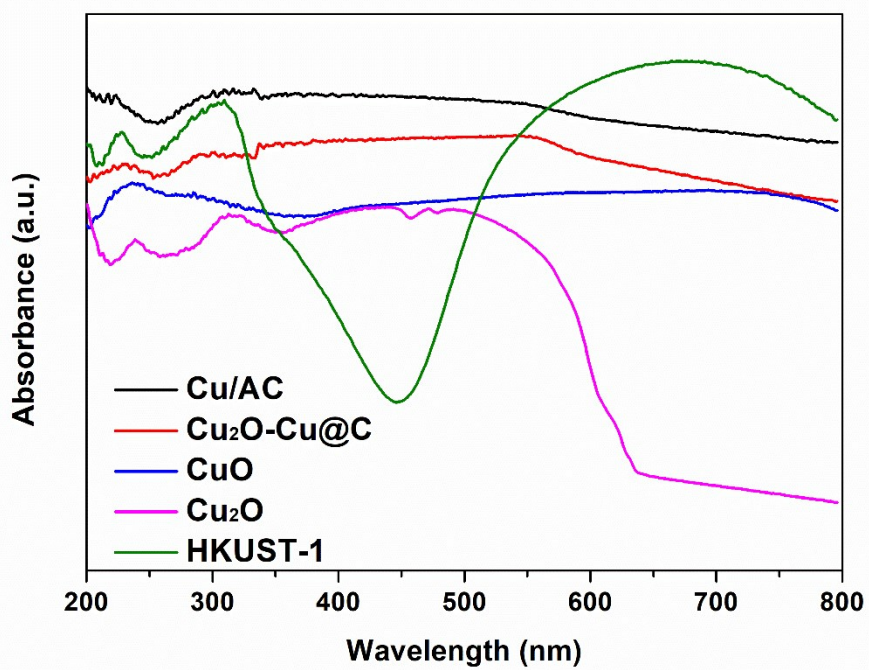


Fig. S10 UV-vis-DR spectra of various samples.

Fig. S11 XRD pattern of Cu/AC.

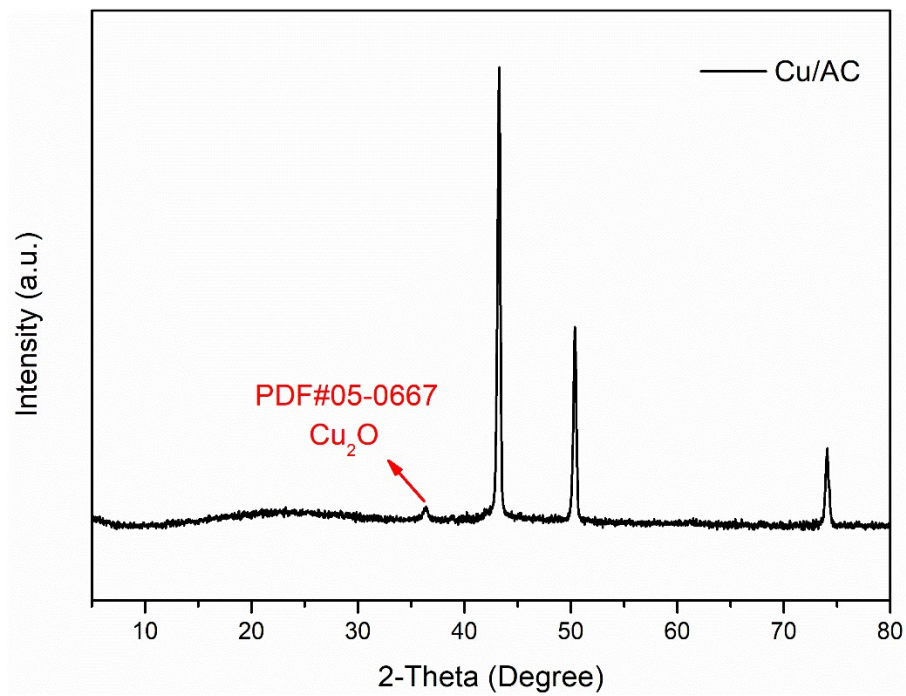


Fig. S11 XRD pattern of Cu/AC.